Mon. Not. R. Astron. Soc. **372,** 1149–1160 (2006) doi:10.1111/j.1365-2966.2006.10911.x

On the mass-to-light ratio of the local Galactic disc and the optical luminosity of the Galaxy

Chris Flynn,[1,3]★ Johan Holmberg,[1,4] Laura Portinari,[1] Burkhard Fuchs[2] and Hartmut Jahreiß[2]

[1]*Tuorla Observatory, Väisäläntie 20, FI-21500 Piikkiö, Finland*
[2]*Astronomisches Rechen-Institut am Zentrum für Astronomie der Universität Heidelberg, Mönchhofstrasse 12-14, Heidelberg, Germany*
[3]*Mount Stromlo Observatory, Weston Creek, ACT, Australia*
[4]*Max-Planck-Institut für Astronomie, Königstuhl 17, Heidelberg, Germany*

Accepted 2006 August 4. Received 2006 August 2; in original form 2006 May 4

ABSTRACT

We measure the volume luminosity density and surface luminosity density generated by the Galactic disc, using accurate data on the local luminosity function and the vertical structure of the disc. From the well-measured volume mass density and surface mass density, we derive local volume and surface mass-to-light ratios (M/L) for the Galactic disc, in the bands B, V and I. We obtain M/L for the local column of stellar matter of $(M/L)_B = 1.4 \pm 0.2$, $(M/L)_V = 1.5 \pm 0.2$ and $(M/L)_I = 1.2 \pm 0.2$. The dominant contributors to the surface luminosity in these bands are main-sequence turnoff stars and giants. Our results on the colours and M/L for the 'solar cylinder' well agree with population synthesis predictions using initial mass functions typical of the solar neighbourhood. Finally, we infer the global luminosity of the Milky Way, which appears to be underluminous by about 1σ with respect to the main locus of the Tully–Fisher relation, as observed for external galaxies.

Key words: Galaxy: disc – galaxies: fundamental parameters.

1 INTRODUCTION

The mass-to-light ratio (M/L)[1] is an important constraint for studies of stellar populations and for chemo-photometric models of the Milky Way; these often serve as a calibration point for the modelling of disc galaxies in general (e.g. Boissier & Prantzos 1999). The surface luminosity and mean colours of the solar column are also useful comparison points in extragalactic studies, and for placing the Milky Way on the Tully–Fisher (TF) relation.

Studies of the Galactic disc over the last two decades have resulted in good determinations of its local mass density $\rho(0)$, and the surface mass density, Σ_0 (e.g. Holmberg & Flynn 2000, 2004, and references therein). In this paper we study the related issue of the luminosity generated by the local disc, both in the local volume (i.e. the volume luminosity density) and integrated perpendicularly to the disc in a column (i.e. the surface luminosity density). These quantities allow us to measure the M/L for the local Galactic disc.

Estimating the luminosity surface density (i.e. surface brightness) of the local Galactic disc requires good knowledge of its vertical structure. In this respect, Galactic models have much improved since the 1980s, as a particular result of the *Hipparcos* satellite and star count programmes made with the *Hubble Space Telescope* (*HST*). These data allow us to overcome the main deficiency in earlier studies of the local disc surface brightness and disc M/L; due to the lack of accurate distances to individual stars, the column luminosity (and mass) density had to be recovered via assumptions about the scalelength h_R and scaleheight h_z of the stellar disc, and the results were degenerate with respect to the assumed h_z/h_R ratio. Distances to stars from *Hipparcos* now allow us to determine directly the distribution of stellar scaleheights and measure column densities, merely by 'counting' stars and light at the Galactic poles; h_R is no longer required in the modelling and the degeneracy is broken.

The infrared structure of the Milky Way has been extensively studied in the 1990s, mostly taking advantage of the *COBE*/DIRBE experiment, and is presently well understood (Kent, Dame & Fazio 1991; Dwek et al. 1995; Binney, Gerhard & Spergel 1997; Freudenreich 1998; Bissantz & Gerhard 2002). On the other hand, in the optical, literature estimates of the disc luminosity and M/L can mostly be traced back to work done prior to the launch of both the *Hipparcos* satellite and Space Telescope (see Table 1 for a list of the main references). The time is thus ripe for a redetermination of the M/L of the disc.

In Sections 2 and 3 we determine the disc luminosity and M/L, both locally and in a column at the Sun, for the optical bands B, V and I. In Section 4, we compare our results to theoretical predictions

★E-mail: cflynn@astro.utu.fi

[1]Unless otherwise explicitly stated, this paper always refers to the M/L of stellar matter.

Table 1. Previous determinations of the surface brightness and colours of the local Galactic disc.

Solar cylinder		Disc			Galaxy			
$\mu_B(R_\odot)$	$\mu_V(R_\odot)$	$M_{B,d}$	$M_{V,d}$	$(B-V)_{0,d}$	$M_{B,g}$	$M_{V,g}$	$(B-V)_{0,g}$	References
24.15 ± 0.07		-19.61 ± 0.06		0.40	-20.08 ± 0.04		0.53 ± 0.02	de Vaucouleurs & Pence (1978)
	$\sim$23	-19.9	-20.4	0.45	-20.5	-20.1	0.45	Bahcall & Soneira (1980), Bahcall (1984a,b)
23.3 ± 0.3	22.7 ± 0.2			0.62 ± 0.04				Ishida & Mikami (1982)
23.8 ± 0.1		-20.2 ± 0.2		0.84 ± 0.15	-20.3 ± 0.2		0.83 ± 0.15	van der Kruit (1986)

from population synthesis modelling. In Section 5, we compute the total disc luminosity, for a range of plausible scalelengths, and make some comparisons between the Milky Way and external galaxies. In Section 6 we summarize and discuss our results. The present study focuses on optical bands, and work is underway to extend these measurements to near-infrared (NIR) bands.

2 TWO INDEPENDENT STUDIES

The luminosity of the local Galactic disc has been determined in this paper, by starting with the stellar luminosity function, and computing the total luminosity the stars contribute both locally, and in a column integrated above and below the position of the Sun in the disc. From the total luminosity, and the known disc mass density and surface density, we then derive disc M/L.

Our analysis of the luminosity budget for the disc has been carried out independently by the group working at Tuorla (CF, JH, LP) and the other at Heidelberg (BF, HJ); we shall hereafter refer to the two programmes as the Tuorla and Heidelberg studies. We found out about each other's studies when they were essentially completed, at which point we decided to combine efforts and discuss the results together. As will be seen, the two studies were in excellent agreement.

In the Tuorla study, our approach was to leverage existing work, carried out some years earlier, on the mass density of the disc. In Holmberg, Flynn & Lindegren (1997) and Holmberg & Flynn (2000, 2004), we constrained the vertical structure of the disc over a wide range of stellar types, primarily using the *Hipparcos* and Tycho surveys. It was relatively straightforward to use those calibrated models of the local Galactic disc to derive its volume and surface luminosity density.

The Heidelberg study is based on very extensive work on the local stellar luminosity function obtained from the CNS4 (Catalogue of Nearby Stars). The high-quality colour, luminosity and velocity data for the sample stars were used to compute the volume luminosity density and surface luminosity density of the disc.

The essential difference between the two studies is that the Tuorla sample reaches to more luminous stellar types, because it surveys a deeper volume (that probed by *Hipparcos*/Tycho out to $\sim$200 pc); and involves a model of the local disc structure. The Heidelberg study reaches to much lower luminosity stars, and is limited to a distance of 25–50 pc from the Sun; furthermore, it is based on completely empirical local stellar data and relies on no modelling. The agreement between the Tuorla and Heidelberg studies, where they overlap, turned out to be excellent, and we have combined the results of the studies with confidence.

2.1 The Tuorla study

The disc luminosity calculations in the Tuorla study are based on a description of the local disc (Holmberg & Flynn 2000, 2004),

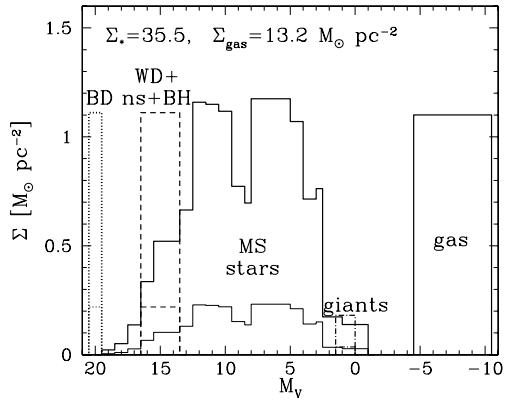

Figure 1. The disc mass model. For each component of the model, the total contribution by mass is shown as a function of the V-band absolute magnitude. MS stands for main sequence, WD + ns + BH for white dwarfs, neutron star and black hole type stellar remnants (their luminosity is dominated by the WDs), BD for brown dwarfs. 'Giants' are first ascent and helium core burning stars of about a solar mass. Thick lines show the total mass contribution (thin + thick disc), thin lines show the thick disc fraction. Note that the gaseous components have been included on the right hand side of the figure (gas), but do not generate optical luminosity). Full details of the model, represented graphically here, are in Table 2. The mass model actually assigns one single value to the global surface mass density in M dwarfs ($M_V > 8$), based on *HST* studies; for the sake of this plot, such global mass in faint stars has been distributed in magnitude following the mass function of Binney & Merrifield (1998).

composed of both gaseous and stellar components, and constructed for the purpose of determining the vertical mass distribution of the disc.

Fig. 1 shows the mass contributions made by the components of the model for the disc. It is an updated version of the mass model of Holmberg & Flynn (2000), and is shown in Table 2. Full details of how these models are constructed can be found in Holmberg & Flynn (2000, 2004). The models consist of a thin disc and a thick disc (and a stellar halo as well, although this is irrelevant in the present study).

The stellar components of the model consist, broadly speaking, of main-sequence stars of different M_V (indicated by MS in Fig. 1), red giants (i.e. first ascent and He core burning giants of about a solar mass), supergiants (i.e. relatively massive, luminous giants), white dwarfs/neutron stars/black holes (i.e. stellar remnants, indicated by WD + ns + BH) and brown dwarfs (indicated by BD in the figure). The scaleheights (i.e. the density falloff with vertical height above the disc) of each stellar component have been constrained by star count data from the *Hipparcos* and Tycho catalogs (for stars brighter than M dwarfs), or via Space Telescope (for the M dwarfs). The scaleheights for stars dimmer than the main-sequence turnoff are mainly constrained by self-consistency with the mass model

Table 2. The disc mass model. Mass components in the disc consist broadly of gas, main-sequence stars and giants, stellar remnants and substellar objects. For each component, the table gives the local mass density at the Galactic mid-plane $\rho(0)$, the vertical velocity dispersion σ_W, and the surface mass density, Σ.

Description	$\rho(0)$ ($M_\odot$ pc^{-3})	σ_W (km s^{-1})	Σ ($M_\odot$ pc^{-2})
H_2	0.021	4.0	3.0
H I(1)	0.016	7.0	4.1
H I(2)	0.012	9.0	4.1
Warm gas	0.0009	40.0	2.0
Giants	0.0006	20.0	0.4
$M_V < 2.5$	0.0031	7.5	0.9
$2.5 < M_V < 3.0$	0.0015	10.5	0.6
$3.0 < M_V < 4.0$	0.0020	14.0	1.1
$4.0 < M_V < 5.0$	0.0022	18.0	1.7
$5.0 < M_V < 8.0$	0.007	18.5	5.7
$M_V > 8.0$	0.0135	18.5	10.9
White dwarfs	0.006	20.0	5.4
Brown dwarfs	0.002	20.0	1.8
Thick disc	0.0035	37.0	7.0
Stellar halo	0.0001	100.0	0.6

(via their known velocity dispersions and the Poisson–Boltzmann equation).

In this model, the surface mass density in stars is $\Sigma_* = 35.5\,M_\odot$ pc^{-2} and for the gaseous components, the surface mass density is $\Sigma_{\rm gas} = 13.2\,M_\odot$ pc^{-2}.

For the stellar components in the model, we have computed how much light is contributed to the local volume and local column. In the V band, this is straightforward, as all the stellar components in the model have well-measured absolute V-band luminosity, M_V, either from space-based parallax data (i.e. *Hipparcos*, for $M_V < 8$) or ground-based parallax data (for $M_V > 8$).

To convert the V luminosities to other bands (B and I), we used the $(B-V)$ and $(V-I)$ colour distributions in the *Hipparcos* and Tycho catalogues. Only directly measured, 'a'-flagged ($V - I_c$) colours were considered, for homogeneity and accuracy. The transformations are very similar to what can be obtained from the collated *UBVRI* data for nearby stars with very accurate parallaxes (Reid 2005, NSTAR catalogue, private communication).

To translate magnitudes to luminosities we adopt a V-band absolute magnitude for the Sun of $M_{V,\odot} = 4.82$; for the other bands we adopt the solar colours from Holmberg, Flynn & Portinari (2006), $(B-V)_\odot = 0.64$ and $(V-I)_\odot = 0.69$.

2.2 The Heidelberg study

At Heidelberg, the disc luminosity density was computed in a slightly different manner. The starting point was the local disc luminosity function, obtained from the CNS4 (Catalogue of Nearby Stars). This represents a census of stars within 25 pc (Jahreiß & Wielen 1997), extending to a 50-pc volume for the brightest stars (Jahreiß, Wielen & Fuchs 1998, Table 3). The CNS4 is complete within 25 pc for stars of spectral type K and earlier, but for later spectral types only in smaller counting volumes. The luminosity function constructed from the star counts has been carefully corrected for this incompleteness (Jahreiß & Wielen 1997).

Estimating the local luminosity density from the LF is straightforward. For the surface luminosity density we proceeded as follows.

Table 3. Luminosity function from the 50-pc sample of the CNS4 catalogue, improving and extending the luminosity function of Jahreiß & Wielen (1997) in the brightest luminosity bins. Φ is expressed in terms of number of stars within a 20-pc volume; ϵ_Φ is the Poisson error; Φ(MS) refers to main-sequence stars only.

M_V	N_{50}	N_{50}(MS)	Φ	ϵ_Φ	Φ(MS)
–3	1	1	0.06	0.06	0.06
–2	–	–	–	–	–
–1	17	9	1.1	0.3	0.6
0	51	26	3.3	1.5	1.7
1	176	96	11.3	0.9	6.1
2	261	224	16.7	1.0	14.3
3	552	483	35.3	1.5	30.9

For stars in a given magnitude bin, an observational vertical velocity dispersion σ_W can be obtained directly from the known space velocities (Jahreiß & Wielen 1997). The detection probability of a star in the volume is $P \propto \sigma^{-1}{}_W$ hence each star type is assigned a weight $1/P \propto \sigma_W$ when going from volume to column quantities (cf. Fuchs et al. 2001), that is, for each magnitude bin:

$$\Sigma_{\rm L}(M_V) \propto \rho_{\rm L}(M_V) \times \sigma_W(M_V). \quad (1)$$

We have verified that this relationship holds in realistic discs, by computing $\rho_*(M_V) \times \sigma_W(M_V)$ for each component of the Tuorla disc model, and comparing it to the surface density found for each component after solving for the density falloff of all components fully self-consistently via the Poisson–Boltzmann equations. As can be seen in Fig. 2 the quantities are very closely proportional. Equation (1) is used in the next section to compare the Tuorla and Heidelberg results on surface luminosity density.

Fig. 3 shows the luminosity function from CNS4 (thick lines with error bars) compared to the one used in the Tuorla Galactic model (thin lines); the agreement is excellent, for both main-sequence and giant stars (lower panel, dashed lines). We now compute the luminosity budget for the local disc based on the Tuorla and Heidelberg studies.

2.3 Local disc *V*-band luminosity budget

We begin with the V band, since this computation was most straightforward.

The local volume luminosity density, $\rho_{\rm L}$ in the V band is shown as a function of V absolute magnitude, M_V, in Fig. 4 for the two studies (Tuorla: thin lines; Heidelberg: thick lines with error bars). The top panel shows the total luminosity emitted by each magnitude wide bin from the local stellar luminosity function; we further compare to the volume luminosity density distribution of Binney & Merrifield (1998, dotted line). The Tuorla study is able to constrain the contribution by luminous stars well because it reaches deeper (about 200 pc) compared to the Heidelberg study (which is for local stars out to 25–50 pc). This is why the Heidelberg data reliably probes luminosities only for $M_V \geqslant -1$. For less luminous stars, where we can compare the two studies directly, the agreement is excellent. The luminosity generated for stars with $M_V \geqslant -1$ is $0.045\,L_\odot$ pc^{-3} in the Tuorla study and $0.047\,L_\odot$ pc^{-3} in the Heidelberg study. From the Tuorla study, we derive a total volume luminosity generated for all stars of $\rho_{\rm L} = 0.056\,L_\odot$ pc^{-3}.

One question we wished to address is which stars dominate the luminosity budget, in the volume as well as in the column, and how is this a function of wavelength (or colour band). We examine this

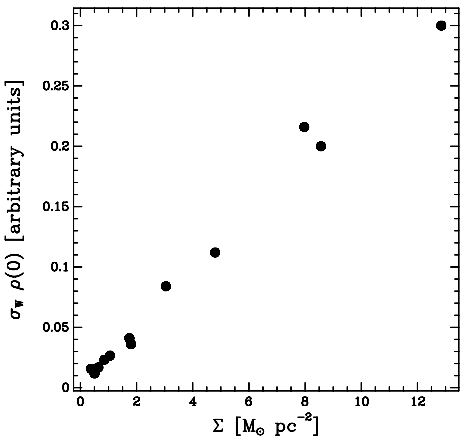

Figure 2. Luminosity function of stars near the Sun, in units of pc^{-3} mag^{-1}. In this and following figures, the thin curve shows the Tuorla study, and the thick curve with error bars the Heidelberg study, the two having been carried out independently. The Tuorla study is based on star counts and fits to the mass distribution of the local Galactic disc due to Holmberg & Flynn (2000), and probes out to 200 pc from the Sun. The Heidelberg study is based on the CNS4 (Catalogue of Nearby Stars), and is limited to stars within 25–50 pc from the Sun. Poisson error bars are shown for the Heidelberg data; the Tuorla error bars are as small or smaller than the Heidelberg ones and are not shown for clarity. Upper panel: total luminosity function; lower panel: luminosity function for main-sequence stars (solid lines) and red giants (dashed lines) separately.

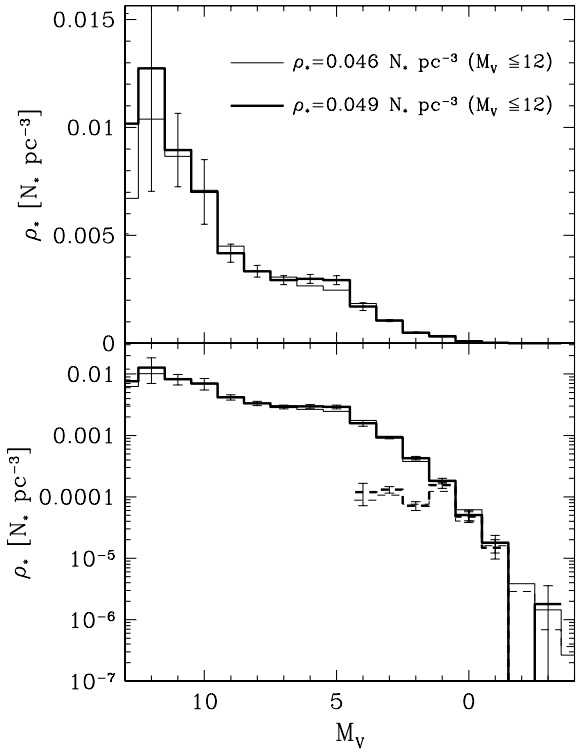

Figure 3. Comparison of the surface density of individual components in our disc models, versus the quantity $\sigma_W \times \rho(0)$ (i.e. the product of vertical velocity dispersion and the density of the component at the disc mid-plane). This shows that equation (1) holds to a very good approximation for realistic discs.

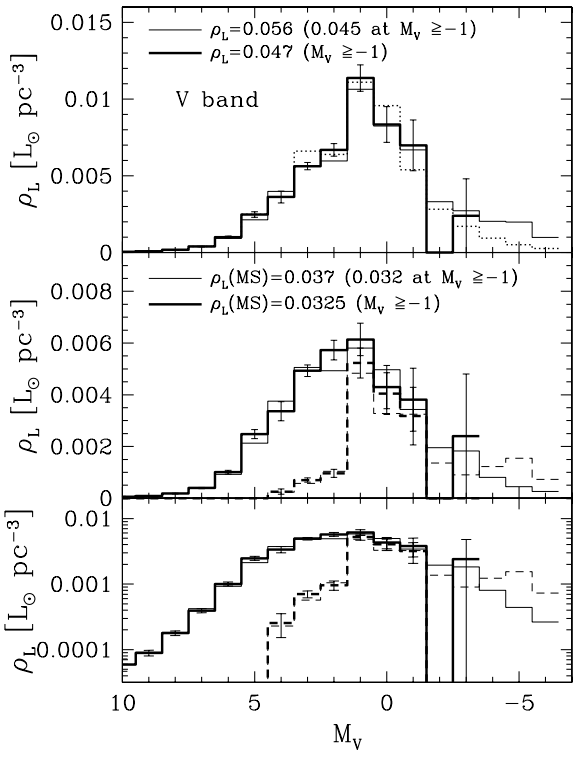

Figure 4. Luminosity generated by stars in the V band near the Sun, in units of L$_\odot$ pc^{-3} mag^{-1}; as in Fig. 3, thin curves for the Tuorla study, thick curves with error bars for the Heidelberg study. Top panel: total V-band luminosity budget, peaking in the local volume in the range $-1 < M_V < 4$; also shown as a dotted line is the V-band luminosity distribution of Binney & Merrifield (1998). Middle and bottom panels: luminosity budget separated into main-sequence (solid lines) and giant components (dashed lines); in linear and logarithmic scale, respectively.

question by dividing the samples into main-sequence stars and giants and show the results in the middle panel of Fig. 4. The main sequence is represented by the solid lines, while the giants are shown by the dashed lines. There is excellent agreement between the samples; the bottom panel shows the same comparison but in logarithmic scale, to highlight the excellent agreement down to the very faint main sequence.

Fig. 4 shows clearly, and not surprisingly, that the main contributors to the local V-band volume luminosity budget are the main-sequence stars around the turnoff, in the range $3 < M_V < 0$; giants contribute mainly in the range $1 < M_V < 0$ (location of the red clump).

The results so far have been for volume luminosity density, ρ_L. More interesting, from the point of view of studies of external galaxies, is the surface luminosity density Σ_L, to which we now turn.

In the Tuorla study, we sum the total contribution of thin and thick disc components in the model by integrating in z, that is, vertically in both directions out of the disc, and accounting for the known falloff of the stars as a function of height. In Fig. 5 we overplot the volume and column luminosity densities for the Tuorla Galactic model. The total luminosity of the column, from the Tuorla data, is $\Sigma_L = 24.4\,L_\odot\ pc^{-2}$.

The comparison to the Heidelberg results is possible via the 'scaled' surface luminosity of equation (1), namely using the vertical velocity dispersion of the stars as a proxy for their scaleheight in the potential; we have shown in Fig. 2 that this is an excellent approximation in the Tuorla Galactic model.

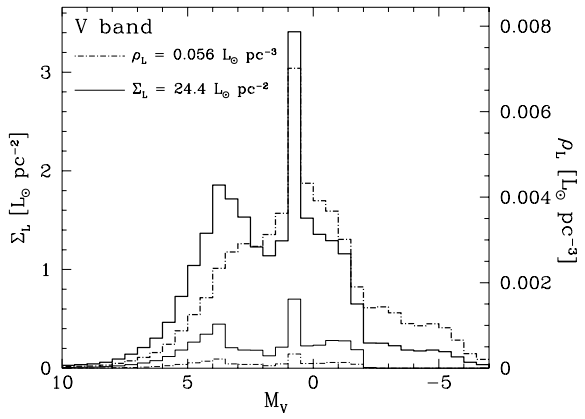

Figure 5. *V*-band luminosity density from the Tuorla disc model in the solar volume (dash–dotted line) and column (solid line); thick histograms for the total (thin + thick) disc, thin lines for the thick disc fraction. In the surface luminosity density, two clear peaks are seen in the luminosity contribution corresponding to turnoff main-sequence stars and to clump giants.

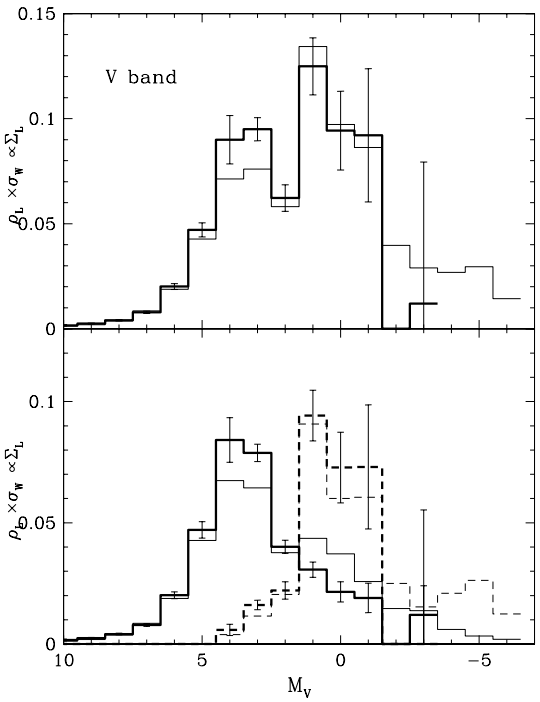

Figure 6. Luminosity budget for the local disc in the *V* band, shown by surface density rather than volume density. We have used $\rho_L \times \sigma_W$ as a proxy for Σ_L, as discussed in the text. There is good agreement between the two data sets. The Tuorla study results in a total *V*-band surface luminosity of $\Sigma_L = 24.4\,L_\odot$ pc^{-2}. Bottom panel: main-sequence (solid) and giant stars (dashed) separately. The two peaks in the luminosity contribution, due to turnoff stars ($M_V \approx 3$–4) and giants (mainly around $M_V \approx 0.5$), separate out clearly. In the *V* band, these two components contribute about equally to the total light.

In the Heidelberg study, we adopt for main-sequence stars the velocity dispersions of Jahreiß & Wielen (1997), and we further assign $\sigma_W = 23$ km s^{-1} to old giants and 12 km s^{-1} to clump giants (which are about half of the giants in the magnitude bins $M_V = 0$–1; Jahreiß, Fuchs & Wielen 1999). Relatively low velocity dispersions for a significant fraction of red giants were found also by Flynn & Fuchs (1994); indeed synthetic Hertzsprung–Russel (HR) diagram analysis shows that the majority of clump giants in the local volume is expected to be as young as 1–2 Gyr (Girardi & Salaris 2001).

Fig. 6 clearly shows very good agreement between the two studies also in the surface brightness estimate: the predicted overall surface luminosity from stars with $M_V \leqslant -1$ (the common magnitude range in the two studies) agrees to better than 10 per cent, with the agreement as good as a few per cent for the MS star contribution, and within 15 per cent for the giant contribution when considered separately.

Turning now to dominant contributors to the luminosity budget, Figs 5 and 6 again show that the luminosity comes mainly from stars in the range $4 < M_V < 0$ – that is, from turnoff stars, and from red giants near the 'clump', as we shall see in more detail below. The contribution from stars brighter than absolute magnitude $M_V = -1$, that is, very bright main-sequence stars and giants, is only $2.3\,L_\odot$ pc^{-2} – or about 10 per cent of the total light in the column. This is a good deal less than the 20 per cent quota they contribute to the volume luminosity (cf. solid versus dot–dashed line in Fig. 5) their contribution being suppressed in the column because bright young MS stars have low velocity dispersion and low scaleheight in the disc.

The bottom panel in Fig. 6 shows the luminosity separated in main-sequence and giant contributions. The dominant part of the luminosity, in the range $4 < M_V < 0$, is now seen to separate into two clean peaks – one due to turnoff stars at $M_V \approx 3$–4 and the other due to giants (primarily 'clump' giants, or core helium burning stars), at $M_V \approx 0.5$. In the *V* band, the two contribute about equally (60–40 per cent, see Table 5) to the surface luminosity density, Σ_L.

The comparison between the Tuorla and Heidelberg results also highlights the importance of the luminosity bins at $M_V = 3$–4: the volume to column transformation gives an important weight to these bins, and the differences in this range between the Tuorla and the Heidelberg results is mainly due to the slightly different σ_W values adopted in the two studies in this range. This is the magnitude range where scaleheight is most rapidly changing with luminosity, and was the part of the Tycho and *Hipparcos* data which had to be fit most carefully (Holmberg et al. 1997). Due to the scaleheight and vertical velocity dispersion effect, when going from volume to column luminosity density, the peak of the MS stars luminosity contribution indeed shifts from $M_V \sim 2$ (Fig. 4, middle panel) to $M_V = 3$–4 (Fig. 6, bottom panel). Also in Fig. 5, overplotting the volume and column luminosity densities for the Tuorla Galactic model, the peak of the main-sequence contribution at $M_V = 3$–4 emerges in the surface luminosity density.

We now turn to the *M/L* of the disc in the *V* band. The Tuorla Galactic model yields in the local volume a *V*-band luminosity density $\rho_L = 0.056\,L_\odot$ pc^{-3}; the stellar mass density is $\rho_* = 0.042\,M_\odot$ pc^{-3} – this yields a disc *M/L* in the *V* band for the local volume of $(M/L)_V = 0.75\,M_\odot/L_\odot$. The local stellar density is determined by *Hipparcos* data to better than 10 per cent, and 10 per cent is also the typical uncertainty in the luminosity, as estimated from the 'freedom' in adjusting the parameters of the Tuorla model versus all available observational constraints, and also based on the comparison with the independent Heidelberg results (Fig. 4). Adding in quadrature, we estimate the uncertainty in *M/L* as ≈15 per cent.

For the column, the luminosity surface density we derive is $\Sigma_L = 24.4\,L_\odot$ pc^{-2}; the column density of *stellar* matter is $35.5\,M_\odot$ pc^{-2}; thus, the surface *M/L* at the position of the Sun in the disc, in the *V* band, is $(M/L)_V = 1.5\,M_\odot/L_\odot$, again with an uncertainty of the order of 15 per cent.

Table 4. Luminosities and *M*/*L* for the local volume and local column, measured in the bands *B*, *V* and *I*, for the *stellar* material of the disc . The error in the luminosity determinations is ≈10 per cent, while the error in the *M*/*L* is ≈15 per cent. Note well that the *M*/*L* are for disc matter in stellar form – the gaseous components have been explicitly left out. For the local disc, their inclusion increases the *M*/*L* in the local column in all bands by a factor of 1.4, as discussed in Section 2.3; the *M*/*L* increases by a factor of 2.2 in the local volume if the gaseous component is included.

Property	Units	*B*	*V*	*I*
Volume luminosity, ρ_L	$L_\odot$ pc^{-3}	0.074	0.056	0.063
Volume *M*/*L*	$M_\odot/L_\odot$	0.57	0.75	0.67
Surface luminosity, Σ_L	$L_\odot$ pc^{-2}	25.60	24.35	29.54
Surface mass-to-light ratio	$M_\odot/L_\odot$	1.39	1.46	1.20

In external galaxy studies, the *M*/*L* for all the *visible* matter, that is, including the gaseous component, is often the relevant quantity. Adopting a local gas surface density of 13.2 $M_\odot$ pc^{-2} (uncertain by about 50 per cent, Holmberg & Flynn 2000, and references therein; Table 2), the total surface density of visible baryons comes to $\Sigma_{bar} = 48.7 \pm 7.5\,M_\odot$ pc^{-2} and the corresponding total *M*/*L* increases by a factor of 1.4, to $(M_{bar}/L)_V = 2\,M_\odot/L_\odot$ with an uncertainty of 20 per cent. This applies to the local disc only; whenever possible in external galaxies one considers the stellar and gaseous components separately, as our *M*/*L* estimates can be rigorously applied to the stellar component only and the gas fraction is not universal.

Tables 4 and 5 summarize these results (for *BVI* bands) on the volume and surface brightness and colours for the local thin disc, thick disc and total disc; the percentage of light contributed by main-sequence versus red giant stars; and the stellar mass-to-light ratio (M_*/L) of the solar cylinder.

3 *B*- AND *I*-BAND ANALYSIS

We now proceed to the other bands – *B* and *I*. For the Heidelberg data, the *V*-band luminosity contributed by each magnitude bin was transformed into *B* and *I* using the average colour–magnitude relations from the HR diagram of the CNS4 catalogue. At Tuorla, we transformed the *V*-band luminosity function, to which the *Hipparcos*/Tycho and *HST* star counts had been fit, to other bands via colour–colour relations for stars in the *Hipparcos*/Tycho catalogue, as discussed in Section 2.1.

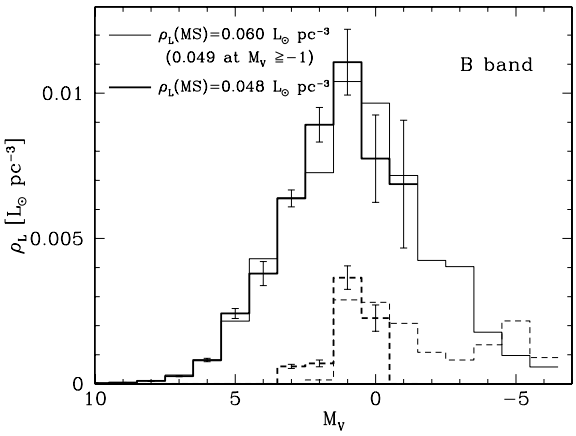

Figure 7. Luminosity density in the local volume in the *B* band. Tuorla results as thin lines, Heidelberg results as thick lines with error bars. There is excellent agreement between the samples for main-sequence stars in the overlapping magnitude range (solid lines); the dashed line is the luminosity contribution from giants in the Tuorla model.

3.1 *B*-band disc luminosity and *M*/*L*

The *B*-band results are shown in Fig. 7. Note that all our results in the non *V* bands are plotted as a function of M_V, to assist comparison with the *V*-band analysis. As before, the Tuorla results are shown by the thin lines and the Heidelberg results the thick lines (with error bars). The total volume luminosity density in the *B* band, as determined from the Tuorla sample, is $\rho_L = 0.074\,L_\odot$ pc^{-3}, most of which (0.06 $L_\odot$ pc^{-3}) from main-sequence stars. Up to $M_V = -1$, the Tuorla and Heidelberg results for MS stars can be compared; the luminosity density up to this point in the Heidelberg sample is $\rho_L = 0.048\,L_\odot$ pc^{-3}, in excellent agreement with the Tuorla estimate. The luminosity contributed by giants in *B* band is less than 20 per cent (Table 5).

The main luminosity contributor in the local volume in the *B* band is from stars at $M_V \approx 1$. Interesting results emerge when the surface luminosity is computed, as seen in Fig. 8. We show only the Tuorla data for clarity and completeness, as the Heidelberg sample does not probe the luminosity function deeply enough. The upper set of curves show both disc components (thin + thick), while the lower set (thin lines) shows the thick disc only. The dash–dotted curves show the volume luminosity density (ρ_L); the solid curves show the surface luminosity density (Σ_L). As in the *V* band, there are two

Table 5. Results of the Tuorla study for the volume and column luminosity and colours of the local thin, think and total disc. The percentage of luminosity contributed by main-sequence stars is also indicated in parenthesis, the rest being due mostly to giants.

Property	Thin disc	Thick disc	Total
ρ_B ($L_\odot$ pc^{-2})	0.072 (82 per cent)	0.002 (53 per cent)	0.074 (81 per cent)
ρ_V ($L_\odot$ pc^{-2})	0.054 (67 per cent)	0.002 (41 per cent)	0.056 (66 per cent)
ρ_I ($L_\odot$ pc^{-2})	0.060 (43 per cent)	0.003 (29 per cent)	0.063 (43 per cent)
Σ_B ($L_\odot$ pc^{-2})	22.10 (82 per cent)	3.50 (53 per cent)	25.60 (78 per cent)
Σ_V ($L_\odot$ pc^{-2})	19.92 (64 per cent)	4.43 (41 per cent)	24.35 (60 per cent)
Σ_I ($L_\odot$ pc^{-2})	22.90 (48 per cent)	6.64 (29 per cent)	29.54 (43 per cent)
μ_B (mag as^{-2})	23.67	25.67	23.51
μ_V (mag as^{-2})	23.14	24.78	22.93
μ_I (mag as^{-2})	22.30	23.65	22.03
$(B-V)_\rho$	0.32	0.89	0.34
$(V-I)_\rho$	0.81	1.13	0.82
$(B-V)_\Sigma$	0.53	0.89	0.58
$(V-I)_\Sigma$	0.84	1.13	0.90

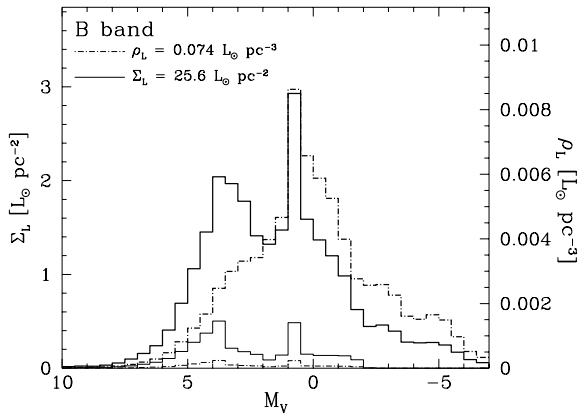

Figure 8. Same as Fig. 5, in the *B* band. Turnoff stars dominate the budget in the *B* band, with the giants providing only 26 per cent of the light, whereas the two components make about equal contributions to the luminosity in the *V* band.

clear peaks in the surface luminosity contribution – one at $M_V \approx 1$ due to clump giants and bright main-sequence stars and the other from turnoff stars ($M_V \approx 4$). Giants contribute only 26 per cent of the surface luminosity in *B*; in this band, turnoff and bright main-sequence stars provide most of the luminosity; in the *V* band instead the proportion is 40–60 per cent.

We obtain a volume luminosity density in *B* of $\rho_L = 0.074\,L_\odot$ pc^{-3}; with a stellar mass density of $\rho_* = 0.042\,M_\odot$ pc^{-3} this yields $(M/L)_B = 0.6$ for the local volume. For the column, the *B*-band luminosity surface density is $\Sigma_L = 25.6\,L_\odot$ pc^{-2}; the stellar mass column density is $35.5\,M_\odot$ pc^{-2}; hence the surface *M/L* in the *B* band for stellar matter is $(M/L)_B = 1.4$. As before, the error on the *M/L* is ≈15 per cent, and the *M/L* is higher by a factor of 1.4 if one includes both stellar and gaseous disc matter in the surface column density (cf. Section 2.3).

3.2 *I*-band disc luminosity and *M/L*

The results for the *I* band are shown in Fig. 9. As with the *B* band, the results are plotted as a function of M_V. For the Heidelberg sample, colour transformations from *V* to *I* were possible for giants only up to $M_V = 0$. Both for the light contributed by MS stars and giants, once more there is excellent agreement (within 10 per cent) between the overlapping parts of each study.

The total volume luminosity density in the *I* band is $\rho_L = 0.063\,L_\odot$ pc^{-3} (this can be computed from the Tuorla sample only).

Again, interesting results emerge when the surface luminosity is computed, as seen in Fig. 10. We show only the Tuorla data for clarity and completeness; line symbols are as in Figs 5 and 8. Two clear peaks in the surface luminosity contribution are seen again – one from giants (mainly clump giants at $M_V \approx 1$) and the other from turnoff stars ($M_V \approx 4$). Also, brighter and redder giants, at $M_V \approx -1$ are starting to contribute to the luminosity. Giants now start to dominate the luminosity budget, contributing more than half (56 per cent) of the total light.

Summarizing the *I*-band results and *M/L*: we obtain a volume luminosity density in *I* of $\rho_L = 0.063\,L_\odot$ pc^{-3}; the stellar mass density is $\rho_* = 0.042\,M_\odot$ pc^{-3} – this yields an *I*-band mass-to-light ratio of $(M/L)_I = 0.7$ for the local volume. For the column, the *I*-band luminosity surface density is $\Sigma_L = 29.5\,L_\odot$ pc^{-2}; the mass column density is $35.5\,M_\odot$ pc^{-2}; hence the surface mass-to-light ratio in the *I* band is $(M/L)_I = 1.2$ in the column. The error on the

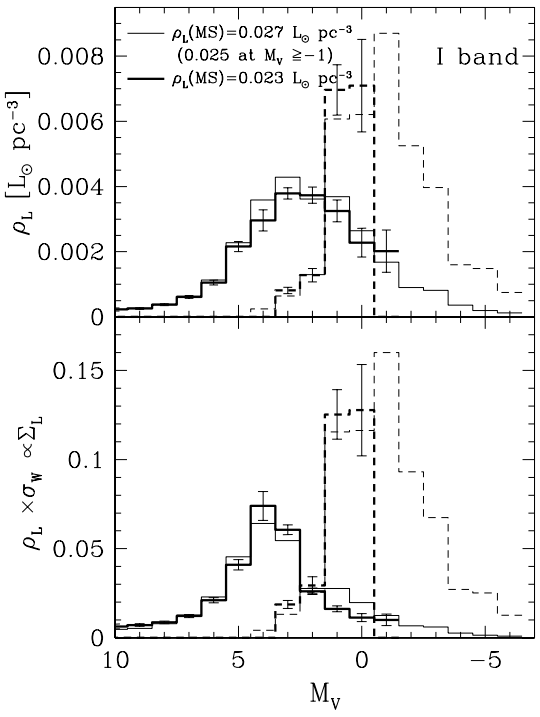

Figure 9. Luminosity density in the *I* band for the local volume (top panel) and column-scaled (bottom panel). Tuorla results as thin lines, Heidelberg results as thick lines with error bars. Solid lines are for MS stars, dashed lines for giants. The total *I*-band luminosity generated locally, from the Tuorla results, is $\rho_L = 0.063\,L_\odot$ pc^{-3}.

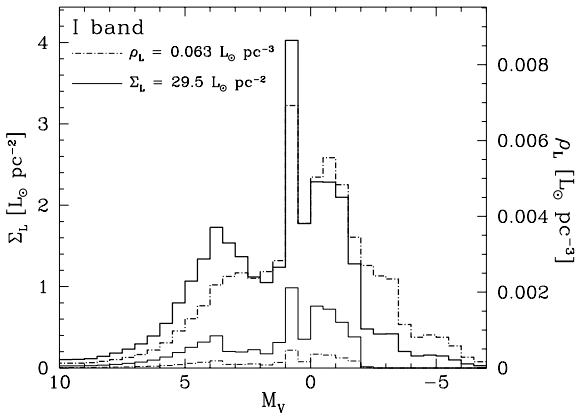

Figure 10. Same as Fig. 5, but in *I* band. Two clear peaks, associated with turnoff stars and clump giants are again seen. The contribution of brighter giants, at around $M_V = -2$, is also starting to have an impact, as one moves to redder bands. In fact, in the *I* band in the solar column, the giants now contribute more than half the light (56 per cent).

M/L is ≈15 per cent, and, as before (Section 2.3) the *M/L* is higher by a factor of 1.4 if one includes both stellar and gaseous disc matter in the local column surface density.

As expected, the analysis showed that relative contributions by the two main factors in the luminosity changes with colour band. In terms of the surface luminosity Σ_L, giant stars contribute about 26 per cent of the light in the *B* band, 40 per cent in *V* band and 56 per cent in *I* band, while only contributing about 0.5 per cent of the stellar surface mass density. Turnoff stars contribute significantly to

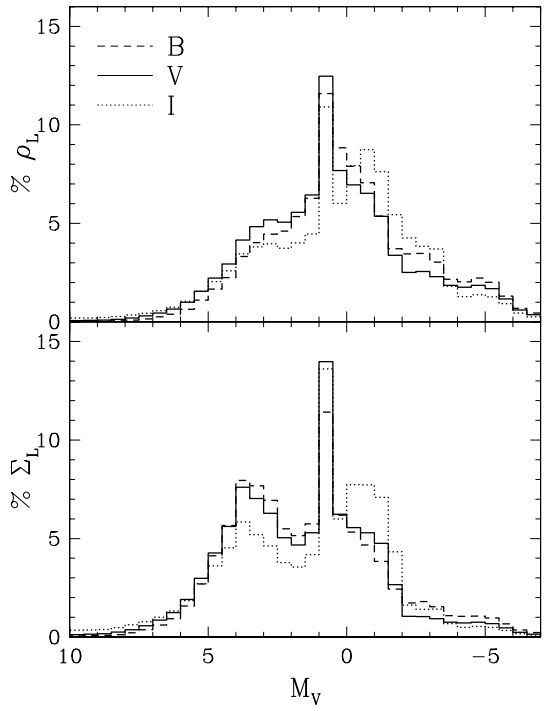

Figure 11. Percentage contribution to volume (upper panel) and column (lower panel) luminosity density in B, V, I band from stars of different magnitude M_V, for the Tuorla disc model.

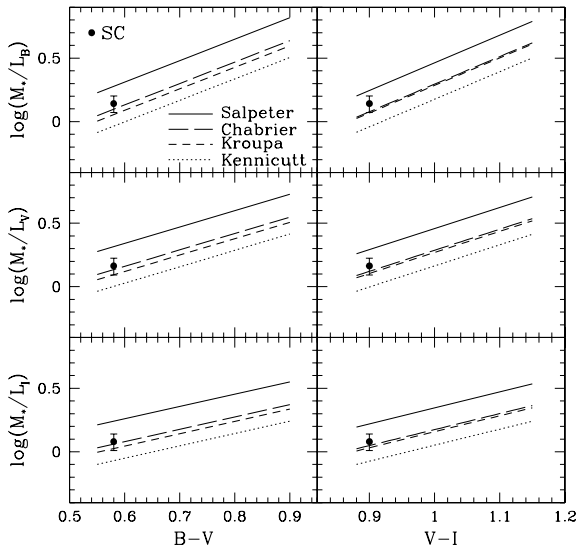

Figure 12. Location of the solar cylinder with respect to the colour–M_*/L relations predicted by stellar populations synthesis models for different IMFs. The results from the Tuorla Galactic model match very well with the theoretical predictions for the Kroupa and Chabrier IMFs, which are representative of the solar neighbourhood.

the light in all bands, while upper main sequence and supergiants ($M_V < -1$) contribute very little to light in all bands.

Finally, in Fig. 11 we compare the luminosity histograms in B, V, I (in units of percentage contribution to the total volume/column luminosity) to highlight how the proportion between the to peaks, of main-sequence stars and giants, changes in different bands.

4 COMPARISON WITH THEORY

Population synthesis models predict well-defined relations between the colours and the stellar mass-to-light ratio (M_*/L) of composite stellar populations, with a zero-point depending on the assumed stellar initial mass function (IMF; Bell & de Jong 2001; Portinari, Sommer-Larsen & Tantalo 2004). Fig. 12 compares our results for the solar cylinder to the theoretical relations by Portinari et al. (2004) computed for different IMFs. The classic Salpeter IMF (extended down to 0.1 $M_\odot$, see Portinari et al. 2004) predicts in this comparison a too large M_*/L – but see below – while the Kennicutt IMF is too 'light'. Our (SC) values are instead in very good agreement with the predictions for the Kroupa (1998) and Chabrier (2001) IMFs, which were derived from solar neighbourhood studies – a successful consistency check.

Of course, both the derivation of the stellar IMF in the local field and our estimate of the surface brightness and colours, ultimately rely on the same type of data, namely star counts in the solar neighbourhood; yet the comparison is not just tautological, as on one hand we have star counts analysed and reproduced with a calibrated model for the vertical structure of the disc, on the other hand the results of population synthesis models assuming an IMF like the local one. And the mass and luminosity contributions are fairly independent, coming from stars of very different magnitude ranges, as apparent by comparing Fig. 1 (mass distribution) to Fig. 4 through 10 (luminosity distributions), the mass and luminosity contributions are fairly independent, coming from stars of very different magnitude ranges.

In the previous sections and in Table 4 the stellar M_*/L was determined on the base of the 'counted' stellar material, with a surface density of $\Sigma_* = 35.5\,M_\odot\,pc^{-2}$ according to the Tuorla mass model; the total surface density of baryons, including the gas component, is about $49\,M_\odot\,pc^{-2}$ (see Fig. 1). This is in good agreement with the dynamical estimates of the surface density of the local disc by, for example, Kuijken & Gilmore (1991), Flynn & Fuchs (1994), Bienaymé et al. (2006). It is also compatible, though on the lower end of the uncertainty range, with the more recent, *Hipparcos*-based dynamical estimate of the surface density $56 \pm 6\,M_\odot\,pc^{-2}$ (Holmberg & Flynn 2000, 2004). This was derived under the assumption of a spherical dark halo; if the halo is somewhat flattened the surface density is lower, since dynamically the best determined quantity is $K_{1.1}$, that is, the total vertical force within 1.1 pc of height on the Galactic plane, while the disc surface density is a derived quantity depending on the adopted dark halo model. The halo of the Milky Way is close to spherical (Ibata et al. 2001; Johnston, Law & Majewski 2005; Belokurov et al. 2006), but the issue is still debated and an axis ratio of 0.7 may be compatible with the data (Ibata et al. 2001; Helmi 2004; Martínez-Delgado et al. 2004). So we can consider 56 ± 6 as an upper limit to the total surface density, which allows for at most 6–12 $M_\odot\,pc^{-2}$ not 'seen' in the visible baryons. By imputing *all* of that to undetected extra stellar matter – and not, for instance, to uncertainties/errors in the gas contribution (which indeed are about 50 per cent), or to a minor dark matter component – the stellar surface density would increase from ∼36 to 42–48 $M_\odot\,pc^{-2}$, and M_*/L would increase by 15–30 per cent over the values given in Table 4. We note that 30 per cent is about the difference between the M_*/L ratios typical of a Kroupa/Chabrier IMF and a Salpeter IMF (see fig. 12 and e.g. fig. 4 in Portinari et al. 2004). The Salpeter scaling can thus be seen as corresponding to the maximum upper limit to M_*/L allowed by the dynamical mass estimates in the solar neighbourhood.

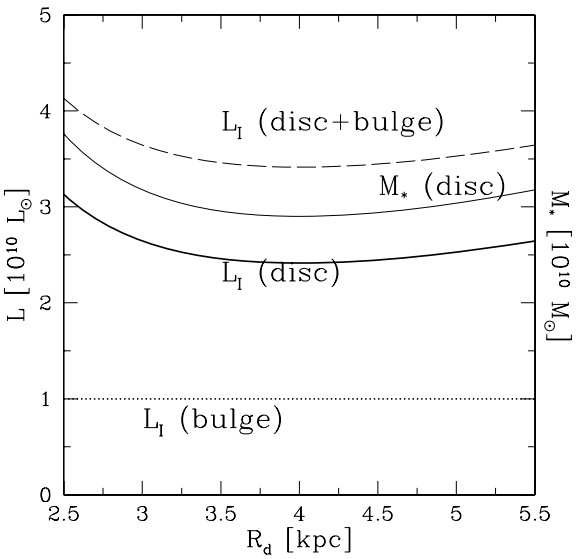

Figure 13. Total *I*-band luminosity of the Milky Way inferred as a function of the assumed disc scalelength, $R_{\rm d}$. The total luminosity is fairly insensitive to the adopted scalelength, at least in the range 2.5–5 kpc.

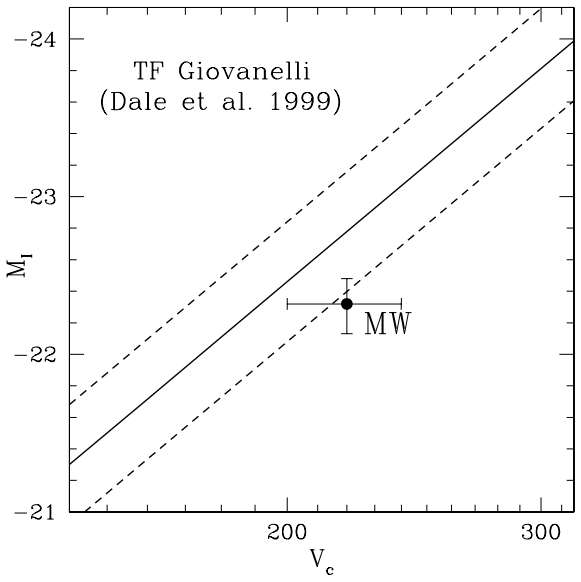

Figure 14. Location of the Milky Way with respect to the *I*-band TF relation (solid line). The dashed lines indicate the 1σ scatter in the TF relation.

5 FROM THE SOLAR CYLINDER TO THE MILKY WAY

From the surface luminosity (or density) at the solar radius one can infer the total luminosity (or mass) of the Galactic disc by assuming an exponential radial profile for the light (or mass); the result is surprisingly *insensitive* to the assumed scalelength $R_{\rm d}$, for a plausible range of scalelengths (i.e. 2.5–5 kpc; as shown by Sommer-Larsen & Dolgov 2001). The function $L_{\rm disc}(R_{\rm d})$ – or $M_{*,\rm disc}(R_{\rm d})$ – has a very broad minimum around $R_{\rm d} \approx {\rm R}_\odot/2$, and for ${\rm R}_\odot = 8$ kpc its shape is as in Fig. 13.

One caveat we should consider is that the solar cylinder probes an interarm region, so we must allow for the spiral arm contrast in deriving the azimuthally averaged surface brightness at the solar radius. We will hence focus on the *I* band as this is most typical for TF studies, and spiral arms are not expected to be very prominent. From the NIR Galactic model of Bissantz & Gerhard (2002), we estimate that spiral arms enhance by only 10 per cent the azimuthally averaged NIR surface brightness at the solar radius, and by at most 13 per cent the overall disc luminosity (see also Drimmel & Spergel 2001; Gerhard 2002); in the *I* band the effect of spiral arms should be of comparable magnitude as the colour contrast is not significant (Rix & Zaritsky 1995, and references therein; Grauer & Riecke 1998). Fig. 13 thus shows the total *I*-band luminosity and stellar mass of the Galactic disc inferred from the local surface brightness and density, including a 10 per cent correction for spiral arms. The total disc luminosity is $L_{I,\rm disc} \sim 2.5$–$3 \times 10^{10}\,{\rm L}_\odot$.

We must further add the bulge contribution to get the total luminosity of the Milky Way, to be compared to external spirals. The bulge luminosity in the NIR is $\sim 10^{10}\,{\rm L}_\odot$ (Kent et al. 1991; Gerhard 2002); we assume the same value in *I* band, which is probably an overestimate as the bulge is mostly composed of red old populations so its NIR luminosity should be larger in proportion than the *I*-band one. The total *I*-band luminosity of the Milky Way is thus $\sim 3.8 \pm 0.6 \times 10^{10}\,{\rm L}_\odot$ (where the error is estimated adding in quadrature an uncertainty of ± 0.3 from the disc scalelength in Fig. 13 and a 10 per cent uncertainty estimated for our determination of the local surface luminosity in Section 3), corresponding to $M_{\rm I} \sim -22.3$. With a circular speed of $\sim 220 \pm 20$ km s^{-1} (the current IAU standard), the Milky Way turns out to be underluminous with respect to the TF relation defined by external spirals (Fig. 14). Although the discrepancy is not dramatic (about 1σ) when considering the scatter in the TF relation and the errors in the Milky Way values, it may indicate a problem with the zero-point of the TF relation or with the stellar *M/L* of disc galaxies.

5.1 Confirming the offset: stellar/baryonic mass

In this section we show that the offset of the Milky Way from the TF relation is confirmed when considering the TF relation in stellar and baryonic mass.

Fig. 15 shows the stellar mass of the Galactic disc estimated as a function of disc scalelength from our local stellar surface density ($35.5\,{\rm M}_\odot$ pc^{-2}, plus a 10 per cent enhancement due to the

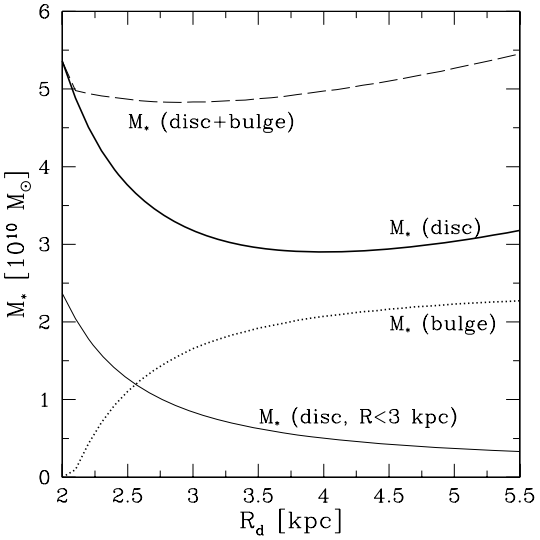

Figure 15. Stellar mass in the disc, bulge and total Milky Way inferred as a function of the assumed disc scalelength, $R_{\rm d}$.

spiral arms on the azimuthal average). For the stellar mass profile scalelengths as short as 2–2.6 kpc have been advocated, based on the global NIR emission or studies of the local stellar distribution (Freudenreich 1998; Vallenari, Bertelli & Schmidtobreick 2000; Bissantz & Gerhard 2002), which correspond to $M_*(\mathrm{disc}) = 3.6$–$5.4 \times 10^{10}\,\mathrm{M}_\odot$. To estimate the bulge mass, we follow Sommer-Larsen & Dolgov (2001) by imposing that the total circular velocity of the bulge + disc combination at 3 kpc does not exceed the observed value of 200 km s^{-1} (Rohlfs et al. 1986). For $R_\mathrm{d} = 2$ kpc, the stellar disc mass enclosed within the central 3 kpc is $2.4 \times 10^{10}\,\mathrm{M}_\odot$, which accounts already for the bulk of the circular velocity with little room for a significant bulge mass. In general, for $R_\mathrm{d} \leqslant 2.6$ kpc, bulge masses of $\leqslant 1.3 \times 10^{10}\,\mathrm{M}_\odot$ at most are compatible with the dynamical constraints. Altogether, the resulting total stellar mass of the Milky Way is 4.85–$5.5 \times 10^{10}\,\mathrm{M}_\odot$ for any $2 \leqslant R_\mathrm{d} \leqslant 5.5$.

The total baryonic mass is obtained by adding the gas mass in the atomic and molecular phases, about $9.5 \pm 3 \times 10^9\,\mathrm{M}_\odot$ (Dame 1993, after applying a 40 per cent correction to account for the mass contribution of helium), out of which $3 \pm 1 \times 10^9\,\mathrm{M}_\odot$ lies within the solar circle. This yields a total baryonic mass for the Milky Way of around $6.1 \pm 0.5 \times 10^{10}\,\mathrm{M}_\odot$, of which $4.9 \pm 0.4 \times 10^{10}$ lies within the solar circle. Our 'back of the envelope' estimate is comparable with the estimate of 5.5×10^{10} (within the solar circle) obtained from full models of the NIR emission and gas dynamics in the Milky Way (Gerhard 2002); the two estimates agree to better than 15 per cent, which we assume to be the error in the total mass estimates.

In Fig. 16 we locate the Milky Way in the observational plane of the stellar mass TF relation; the offset of about 1σ with respect to external galaxies is confirmed. With respect to the baryonic TF relation (McGaugh 2005, fig. 17) the Milky Way lies close enough to the observed relation when stellar masses are estimated on the base of population synthesis models (dashed lines) but the offset is very significant when the stellar M_*/L ratio is assigned with the favoured recipe of minimizing the scatter in the empirical mass discrepancy – acceleration relation (and consequently, in the TF relation itself, see McGaugh 2005 for details; solid lines).

All in all, the offset between the Milky Way and external galaxies is confirmed.

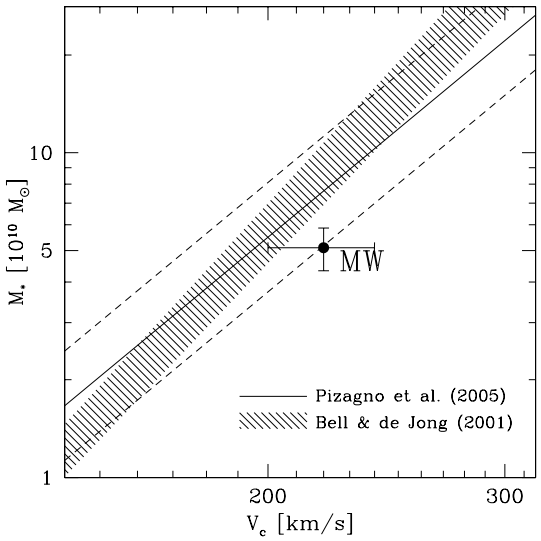

Figure 16. Location of the Milky Way with respect to the stellar mass TF relation.

5.2 Discussion

In the following we discuss possible causes and solutions to this discrepancy.

(i) We took our very local value of the surface brightness to infer the global Milky Way luminosity and mass. The solar neighbourhood is an interarm region and, although we did correct for spiral arm enhancement relying on the current understanding of the spiral structure of the Milky Way, it is possible that the correction is underestimated. In fact, current models indicate for the Milky Way significantly weaker spiral arms than is typical for other spiral galaxies in *K* band (Rix & Zaritsky 1995; Drimmel & Spergel 2001; though Seigar & James 1998 also indicate an average arm strength of 10 per cent); hence we might be presently underestimating the fraction of light in spiral arms for our own Galaxy.

Conversely, local enhancements of bright stars such as Gould's Belt or the local arm (Orion Spur), may tend to boost the surface brightness in the solar cylinder – reinforcing the discrepancy with the TF relation. However the Heidelberg sample, limited to the nearest 25–50 pc, is free from such potential 'contaminations' and the excellent agreement between the Tuorla and the Heidelberg results provides a consistency check for magnitudes $M_V \geqslant -1$ (Fig. 9); stars brighter than those in the Tuorla study provide less than 10 per cent of the total *I*-band surface luminosity (Fig. 10) hence we do not expect Gould's Belt or the Orion spur to induce major offsets. Besides, the fact that our stellar M_*/L is in excellent agreement with population synthesis predictions for the local stellar IMF, is an argument against significant local biases.

(ii) The Milky Way may be a redder and earlier type spiral than the Sbc-Sc galaxies typically defining the TF relation, requiring a significant colour correction for the comparison (Kannappan, Fabricant & Franx 2002; Portinari, Sommer-Larsen & Tantalo 2004); however, the disc is locally quite blue ($B - V \sim 0.6$, Table 5) which argues against major colour and M_*/L offsets between the Milky Way and Sbc-Sc spirals, which typically have $B - V \sim 0.55$. Although full chemo-photometric models of the Milky Way are necessary to explore this possibility, the fact that the offset is found also when considering the stellar mass and baryonic TF relation, reinforces the conclusion that it cannot be purely a colour/Hubble type effect.

(iii) From Fig. 13 it is clear that the inferred total luminosity of the disc rises sharply if the radial scalelength is shorter than 2.5 kpc. An *I*-band scalelength as short as 2 kpc would yield a total Milky Way luminosity of $5.5 \times 10^{10}\,\mathrm{L}_\odot$ or $M_I = -22.7$, within 0.1 mag of the TF locus. Scalelengths as low as 2–2.2 kpc have been advocated for the NIR emission and the stellar mass distribution (Section 5.1); however it is likely that in bluer bands, such as *I* band, the scalelength is longer due to the colour gradients typical of Galactic discs (de Jong 1996), and in fact longer scalelengths of 3.5–5 kpc are quoted for, for example, the *B* band (de Vaucouleurs & Pence 1978; van der Kruit 1986).

More importantly, if its *I*-band scalelength were 2 kpc, the Milky Way would be a 1.5σ outlier in the scalelength–V_c relation; for its circular velocity, in fact, external spirals typically have an *I*-band $R_\mathrm{d} = 3.5 \pm 1$ kpc (e.g. fig. 8 in Sommer-Larsen, Götz & Portinari 2003). Therefore the Milky Way, though matching in that case the TF relation, would still be a non-typical spiral galaxy, from a different point of view.

(iv) In Fig. 14 we compare the Milky Way to the TF relation by Dale et al. (1999). Portinari et al. (2004; appendix A) discuss differences and offsets among observational TF relations by different groups. Although lower TF luminosity normalizations do exist in

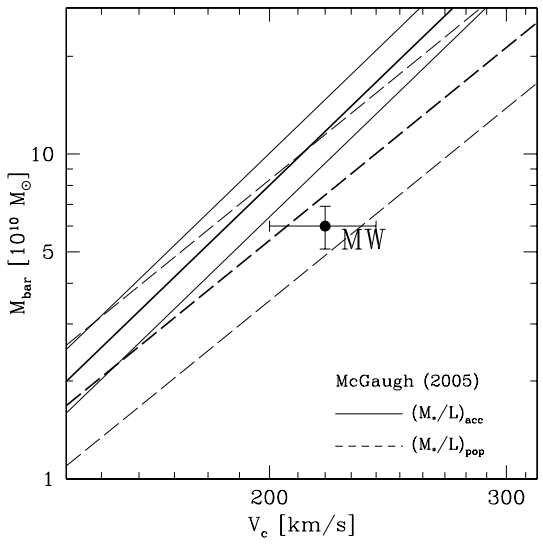

Figure 17. Location of the Milky Way with respect to the baryonic TF relation.

literature, it seems that all the most recent formulations, based on inverse or bivariate fits to the data, are in very good agreement. Especially considering that the new Dale et al. (1999) normalization is 0.1 mag dimmer than the earlier TF by Giovanelli et al. (1997), there is close agreement with the results of, for example, Tully et al. (1998), Tully & Pierce (2000), Courteau et al. (2000). The Cepheid-distance-based TF of Sakai et al. (2000) is steeper than the others, yet this affects only objects of smaller size than the Milky Way, while for $V_c \sim 200$ km s^{-1} the Sakai TF luminosities are similar to the Dale et al. (1999) and other results. Consequently, the discrepancy we found is not just a result of the specific TF data set to which we have compared. Furthermore, the offset is confirmed when considering other TF planes, like the stellar mass and baryonic TF relations (Figs 16 and 17).

(v) The TF relations we considered in the previous item correspond to $H_0 \simeq 70$ km s^{-1} Mpc^{-1}, and/or to the Cepheid *HST* Key-project distance scale. A larger value of H_0, would be required to make external galaxies closer and intrinsically fainter, and reducing the Milky Way's offset from the mean TF. The value of H_0 is still debated on the basis of (i) the Cepheid period-luminosity calibration and its metallicity dependence, (ii) the treatment of extinction and (iii) possible systematic biases and of the comparison to other distance indicators (Sandage et al. 2006, and references therein; Tully & Pierce 2000; Teerikorpi & Paturel 2001; Storm et al. 2005; Ngeow & Kanbut 2006). However, most of the above-mentioned studies point to longer distance scales and lower values of $H_0 \simeq 60$ km s^{-1} Mpc^{-1}, which would increase the offset in Fig. 14. Dimming the TF relation by 0.5 mag in Fig. 14 would require an upward revision of H_0 by 26 per cent, or $H_0 \simeq 90$ km s^{-1} Mpc^{-1}, which looks beyond the plausible range presently discussed (but see Tully & Pierce 2000).

(vi) Finally, the TF relation is so steep ($L \propto V^{\alpha}_c$, with $\alpha = 3$–4) that a small error in the circular velocity will result in a major offset in luminosity. From Fig. 14, one can see that the Milky Way would nicely fall on to the TF relation if its circular speed were as low as $\sim$190 km s^{-1}. Although estimates of the local circular velocity down to 185 km s^{-1} can be found (e.g. Olling & Merrifield 1998; Dias & Lépine 2005), they are at the lowermost end of the plausible range (Sackett 1997; Majewski et al. 2006; and references therein) and seem to be excluded by recent studies of the motion of open clusters (Frinchaboy & Majewski 2006). Besides, direct measurements of the proper motion of Sagittarius A (the Galactic Centre) favour rotation speeds as high as 235 km s^{-1} (Reid & Brunthaler 2004) and even values up to 255 km s^{-1} have been proposed in the literature (Uemura et al. 2000).

Also biases in the observationally determined circular speed of TF spirals are of concern here, and are related to different tracers or definitions of circular velocity. The TF relation by Giovanelli et al. (1997) and Dale et al. (1999) is based on the HI linewidth W_{50}, which corresponds very closely to twice the maximum velocity of the optical disc $V_{max} \sim V_{2.2}$ (Courteau 1997); and the circular speed at the solar radius discussed above cannot be but a lower limit to V_{max} for the Milky Way disc. Hence, though we can expect offsets of order 10 km s^{-1} between $W_{50}/2$ and V_{max} around $V_{max} \sim$ 200 km s^{-1} (Kannappan et al. 2002), the effect does not seem to be large enough to account for the discrepancy in Fig. 14. Besides, as mentioned above, different *I*-band TF relations defined by different groups, with different kinematic tracers (Tully et al. 1998; Dale et al. 1999; Courteau et al. 2000; Sakai et al. 2000) are in very good agreement on the luminosity level of galaxies with Milky Way like rotation velocities.

(vii) Dust is unlikely to be responsible for the discrepancy, since both the TF relation and our Galactic disc model are dust corrected. As our Galactic disc study is based on quite nearby stars, it is hardly plausible that dust corrections have been underestimated by as much as 50 per cent (which is the increase in luminosity required to bring the Milky Way in perfect agreement with the TF relation). Likewise, if dust corrections for external spirals have been systematically overestimated (artificially brightening the zero-point of the TF relation), it is unrealistic that this is by as much as 0.4 mag.

Although many interpretations and possible solutions of the Milky Way's offset relative the mean TF relation have been discussed here, our findings do suggest a possible problem with the luminosity zero-point of the TF relation, and/or with the stellar mass-to-light ratio of disc galaxies. A similar conclusion is suggested also by cosmological semi-analytic models or simulations of galaxy formation (Dutton et al. 2006; Gnedin et al. 2006; Portinari & Sommer-Larsen 2006). The issue certainly deserves further investigation.

6 CONCLUSIONS

We have presented new estimates of the B, V, I luminosity density, colours and M/L of the 'solar volume' and 'solar cylinder', that is, the local Milky Way disc, based on *Hipparcos*/Tycho data and the use of a calibrated model for the vertical structure of the disc to correct from volume to column quantities (the Tuorla study). Excellent agreement is found with the parallel Heidelberg study determining the local luminosity density on completely empirical grounds, based on the complete CNS4 catalogue of nearby stars, at least over the (more limited) magnitude range probed by this latter study.

Our determination of the B, V, I colours and stellar M/L for the solar cylinder is in excellent agreement with theoretical expectations, from stellar population synthesis, for a Kroupa/Chabrier IMF representative of the solar neighbourhood. The uncertainty in the dynamical estimate of the local surface mass density indicate the Salpeter IMF as the extreme upper limit allowed for the local stellar M_*/L; but the Kroupa/Chabrier scaling remains most plausible.

Surface, or column, luminosities and colours provide important constraints for chemo-photometric models of the solar neighbourhood and the Milky Way, and allow us to compare the Milky Way to external spirals. We have reconstructed from the local disc brightness the total *I*-band luminosity of the Milky Way, which appears to be low with respect to the TF relation; although the discrepancy is not dramatic (about 1σ), we discussed the implications and possible ways out. On the other hand, were the Milky Way simply a 1σ outlier from the TF relation (nothing to upset the Copernican principle), it is still worth to underline such offset as our Galaxy is usually taken as the paradigm for disc galaxies in general.

We are presently refining our *I*-band luminosity estimate with the aid of DENIS and other star counts, and defining better our error bars; we are also extending our surface brightness determination to other photometric bands, especially in the infrared utilizing DENIS and 2MASS.

ACKNOWLEDGMENTS

We thank Neill Reid for kindly allowing us to use his *UBVRI* data set on nearby stars and the anonymous referee for helpful comments. We are very grateful to the Academy of Finland for considerable financial support (grants nos 206055 and 208792). LP further acknowledges the support of a EU Marie Curie Intra-European Fellowship under contract MEIF-CT-2005-010884. CF thanks Mount Stromlo Observatory for its kind hospitality, where part of this research was carried out.

REFERENCES

Bahcall J. N., 1984, ApJ, 276, 169
Bahcall J. N., 1984, ApJ, 287, 926
Bahcall J. N., Soneira R. M., 1980, ApJS, 44, 73
Bell E. F., de Jong R. S., 2001, ApJ, 550, 212
Belokurov V. et al., 2006, ApJ, 642, L137
Bienaymé O., Soubiran C., Mishenina T. V., Kovtyukh V. V., Siebert A., 2006, A&A, 446, 933
Binney J. J., Merrifield M., 1998, Galactic Astronomy. Princeton Univ. Press, Princeton, NJ
Binney J. J., Gerhard O. E., Spergel D., 1997, MNRAS, 288, 365
Bissantz N., Gerhard O. E., 2002, MNRAS, 330, 591
Boissier S., Prantzos N., 1999, MNRAS, 307, 857
Chabrier G., 2001, ApJ, 554, 1274
Courteau S., 1997, AJ, 114, 2402
Courteau S., Willick J. A., Strauss M. A., Schlegel D., Postman M., 2000, ApJ, 544, 636
Dale D. A., Giovanelli R., Haynes M. P., Campusano L. E., Hardy E., 1999, AJ, 118, 1489
Dame T. M., 1993, in Holt S. S., Verter F., eds, AIP Conf. Proc. Vol. 27, Back to the Galaxy. Am. Inst. Phys., New York, p. 267
de Jong R. S., 1996, A&A, 313, 45
de Vaucouleurs G., Pence W. D., 1978, AJ, 83, 1163
Dias W. S., Lépine J. R. D., 2005, ApJ, 629, 825
Drimmel R., Spergel D. N., 2001, ApJ, 556, 181
Dutton A., van den Bosch F. C., Dekel A., Courteau S. 2006, ApJ, preprint (astro-ph/0604553)
Dwek E., Arendt R. G., Hauser M. G. et al., 1995, ApJ, 445, 716
Flynn C., Fuchs B., 1994, MNRAS, 270, 471
Freudenreich H. T., 1998, ApJ, 492, 495
Frinchaboy P. M., Majewski S. R., 2006, in de Jong R., ed., Island Universes: Structure and Evolution of Disc Galaxies. Springer-Verlag, Dordrecht, preprint (astro-ph/0508666)
Fuchs B., Dettbarn C., Jahreiß H., Wielen R., 2001, in Deiters S., Fuchs B., Spurzem R., Just A., Wielen R., eds, ASP Conf. Ser. Vol. 228, Dynamics of Star Clusters and the Milky Way. Astron. Soc. Pac., San Francisco, p. 235
Gerhard O. E., 2002, Space Sci. Rev., 100, 129
Giovanelli R., Haynes M. P., Herter T., Vogt N. P., 1997, ApJ, 477, L1
Girardi L., Salaris M., 2001, MNRAS, 323, 109
Gnedin O. Y., Weinberg D. H., Pizagno J., Prada F., Rix H.-W. 2006, ApJ, preprint (astro-ph/0607394)
Grauer A. D., Riecke M. J., 1998, ApJS, 116, 29
Helmi A., 2004, MNRAS, 351, 643
Holmberg J., Flynn C., 2000, MNRAS, 313, 209
Holmberg J., Flynn C., 2004, MNRAS, 352, 440
Holmberg J., Flynn C., Lindegren L., 1997, in Battrick B., Perryman M. A. C., Bernacca P. L., eds, Hipparcos. ESA Publication Division, Noordwijk, ESA SP-402, p. 721
Holmberg J., Flynn C., Portinari L., 2006, MNRAS, 367, 449
Ibata R., Lewis G., Irwin M., Totten E., Quinn T., 2001, ApJ, 551, 294
Ishida K., Mikami T., 1982, PASJ, 34, 89
Jahreiß H., Wielen R., 1997, in Battrick B., Perryman M. A. C., Bernacca P. L., eds, Hipparcos. ESA Publication Division, Noordwijk, ESA SP-402, p. 675
Jahreiß H., Wielen R., Fuchs B., 1998, Acta Historica Astron., 3, 171
Jahreiß H., Fuchs B., Wielen R., 1999, Ap&SS, 265, 247
Johnston K. V., Law D. R., Majewski S. R., 2005, ApJ, 619, 800
Kannappan S. J., Fabricant D. G., Franx M., 2002, AJ, 123, 2358
Kent S. M., Dame T. M., Fazio G., 1991, ApJ, 378, 131
Kroupa P., 1998, in Rebolo R., Martin E. L., Osorio M. R. Z., eds, ASP Conf. Ser. 134, Brown Dwarfs and Extrasolar Planets. Astron. Soc. Pac., San Francisco, p. 483
Kuijken K., Gilmore G., 1991, ApJ, 367, L9
Majewski S. R., Law D. R., Polak A. A., Patterson R. J., 2006, ApJ, 637, L25
Martínez-Delgado D., Gómez-Flechoso M. Á., Aparicio A., Carrera R., 2004, ApJ, 601, 242
McGaugh S. S., 2005, ApJ, 632, 859
Ngeow C., Kanbut S. M., 2006, ApJ, 642, L29
Olling R. P., Merrifield M. R., 1998, MNRAS, 297, 943
Pizagno J. et al., 2005, ApJ, 633, 844
Portinari L., Sommer-Larsen J. 2006, MNRAS, preprint (astro-ph/0606531)
Portinari L., Sommer-Larsen J., Tantalo R., 2004, MNRAS, 347, 691
Reid M. J., Brunthaler A., 2004, ApJ, 616, 872
Rix H.-W., Zaritsky D., 1995, ApJ, 447, 82
Rohlfs K., Chini R., Wink J. E., Böhme R., 1986, A&A, 158, 181
Sackett P. D., 1997, ApJ, 483, 103
Sakai S. et al., 2000, ApJ, 529, 698
Sandage A., Tamman G. A., Saha A., Reindl B., Macchetto F. D., Panagia N. 2006, ApJ, preprint (astro-ph/0603647)
Seigar M. S., James P. A., 1998, MNRAS, 299, 685
Sommer-Larsen J., Dolgov A., 2001, ApJ, 551, 608
Sommer-Larsen J., Götz M., Portinari L., 2003, ApJ, 596, 47
Storm J., Gieren W. P., Fouqué P., Barnes T. G., Gómez M., 2005, A&A, 440, 487
Teerikorpi P., Paturel G., 2001, A&A, 381, L37
Tully R. B., Pierce M. J., 2000, ApJ, 533, 744
Tully R. B., Pierce M. J., Huang J.-S., Saunders W., Verheijen M. A. W., Witchalls P. L., 1998, AJ, 115, 2264
Uemura M., Ohashi H., Hayakawa T., Ishida E., Kato T., Hirata R., 2000, PASJ, 52, 143
Vallenari A., Bertelli G., Schmidtobreick L., 2000, A&A, 361, 73
van der Kruit P., 1986, A&A, 157, 230
van der Kruit P., 1988, A&A, 192, 117

This paper has been typeset from a TEX/LATEX file prepared by the author.